# Elucidation of Binding Sites for Protein Denaturation by Surfactant

ALI A. MOOSAVI-MOVAHEDI* AND ALI A. SABOURY
*Institute of Biochemistry and Biophysics,*
*University of Tehran, Tehran, Iran*

**Summary**: One of the most important lessons that can be learned from studies of protein-surfactant interaction is that the details of the process reflect the detailed tertiary structures of the proteins. The binding of ionic surfactants to different water-soluble proteins; urease, peroxidase, human serum albumin and amino acid oxidase, were extensively studied by equilibrium dialysis and isothermal titration microcalorimetry techniques. The electrostatic interaction, which is accompanied by a preliminary hydrophobic interaction, occurs initially and is followed by a more extensive pure hydrophobic interaction. The predominant unfolding of a protein is related to the first interaction, in which neutralization of charges at the surface of the protein perturb the balance of forces in the protein structure. The number of binding sites in the first set, g1, is markedly consistent with concentration at midpoint of denaturation profiles and very close to the sites at the surface of the single subunit protein with opposite charge with respect to the ionic head group of surfactant.

## Introduction

Denaturation studies are capable of yielding information about the native state in terms of its cooperativity, intrinsic stability, and the nature of the forces required to maintain its tertiary structure [1-5]. Denaturation for providing additional information on the structure, properties, and function of protein can be brought about in many ways[6-8]. These include thermal denaturation, by raising the temperature [9-10], cold denaturation [11], chemical denaturation by urea or guanidinum chloride [12-13], salt denaturation [14], pressure denaturation [6], denaturation by surfactant [15-19], denaturation by solvent [20] and denaturation by pH change [6].

The binding of surfactants with water-soluble proteins has been studied extensively. It is established that surfactants can be broadly divided into those which complex to proteins bring about initiate unfolding of the tertiary structure (denaturing surfactants) and those in which the tertiary structure is maintained (non-denaturing surfactants). The commonly used anionic surfactants, e.g. sodium n-dodecyl sulphate (SDS), or cationic surfactants, e.g. dodecyl trimethylammonium bromide (DTAB), fall into the former category. There are also some proteins which are resistant to denaturation by even powerful denaturants such as SDS under certain conditions, e.g. papain, pepsin and bacterial catalase [21-22], and there are cases of surfactant activation of enzymes, e.g. Aspergillus niger catalase is activated by SDS [23].

The interactions of proteins with ionic surfactants differ from their interactions with other ligands in three important respect:

1. Ionic surfactants having hydrocarbon-chain lengths of eight or more carbon atoms are the most potent protein denaturants known [2,24].
2. Unlike all other classes of ligand, except hydrogen ion, they combine with most native proteins in multiple equilibria, i.e. many equivalents per mole of protein. Surfactants combine in still larger quantities with proteins that have been unfolded [25-26].
3. With respect to the amphipathic nature of surfactants and proteins, it is well established that there are two kinds of interactions in the binding of ionic surfactants to proteins [27]. The binding of the ionic head group of surfactants initially occur to the sites with opposite charge at the surface of the protein followed by more extensive hydrophobic binding to hydrophobic residues in the protein

*To whom all correspondence should be addressed.

[28-29]. Due to this fact, it is expected that there exists at least two sets of binding sites in the protein.

The binding of surfactants to proteins follow the usual thermodynamic laws of equilibrium. Binding is a function of the free surfactant concentration in equilibrium with the protein. It is influenced by temperature, pH, ionic strength and other environmental factors. Analysis of the binding data is usually performed as presented by Scatchard [30-32], Klotz [33-34], Hill [35] and Wyman [36].

In this paper, results are presented that elucidate the binding sites for denaturation of proteins by ionic surfactants and the discussion on mechanism of binding and protein denaturation.

**Results and Discussion**

The interaction of various proteins containing different numbers of subunit with different surfactants is discussed below:

*a) DAO-DTAB Interaction*

DAO is a small globular flavoprotein. It exists in monomeric and dimeric states, based on the enzyme concentration [44-45]. DAO has about 347 residues in its single subunit primary structure [46]. Figure 1 shows the binding isotherm expressed as the number of bound DTAB ions per DAO molecule ($\nu$) as a function of logarithm of free DTAB concentration $[S]_f$ at pH=8.3. The trend of binding can be evaluated by considering it Scatchard plot, which is a plot of $\bar{\nu}/[S]_f$ vs $\bar{\nu}$ and it has been shown inset in Fig. 1. The Scatchard plot is a non-linear and concave unusual shape with a minimum. This unusual behaviour may be interpreted by considering two sets of binding with different affinity. For such system, the binding data can be fitted to Hill equation with more than one term [19].

$$\bar{\nu} = \underbrace{\frac{g_1(K_1[S]_f)^{n_1}}{1+(K_1[S]_f)^{n_1}}}_{\text{first set}} + \underbrace{\frac{g_2(K_2[S]_f)^{n_2}}{1+(K_2[S]_f)^{n_2}}}_{\text{second set}} \quad (1)$$

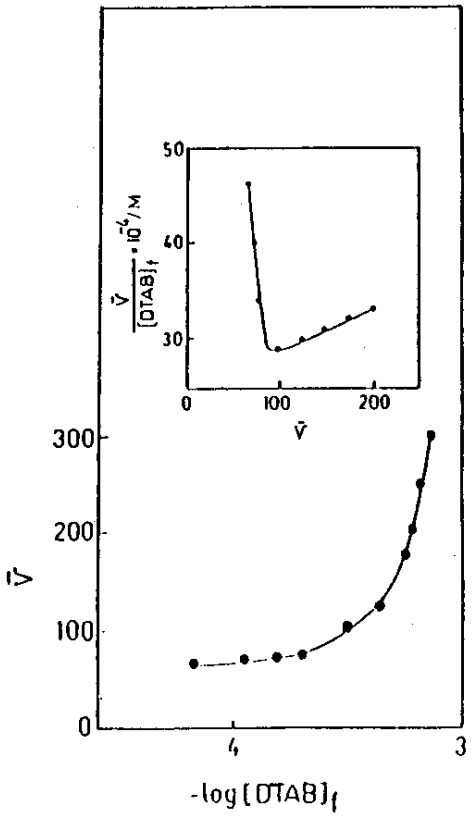


Fig. 1: Binding isotherm for DAO-DTAB interaction at 27°C and pH = 8.3. Insert is Scatchard plot for this system.

where $g_1$, $K_1$ and $n_1$ are the number of binding sites, mean binding constant, and Hill coefficient for first binding set and $g_2$, $K_2$ and $n_2$ are the corresponding parameters for second binding set. Fitting of binding data to the equation (1) has been done by a computer program based on a non-linear least square fitting [47] and the fitting parameters have been shown in Table 1. The first binding set, including electrostatic interaction containing 90 binding sites.

Figure 2 shows the variation in the calorimeteric enthalpy of DAO-DTAB interaction per mole of protein, which has been divided to $\bar{\nu}$, $\Delta H\bar{\nu} = \Delta H/\nu$ with respect to the total concentration of the surfactant. The process is endothermic and the trend of variation shows a maximum at $\bar{\nu}$ = 90 and

Table 1. The value of binding parameters for protein-surfactant interaction at specified pH and temperature of 27°C.

| Interaction | pH | $g_1$ | $K_1/M^{-1}$ | $n_1$ | $g_2$ | $K2/M^{-1}$ | $n_2$ |
|---|---|---|---|---|---|---|---|
| DAO-DTAB | 8.3 | 90 | 19830 | 0.69 | 200 | 1760 | 5.30 |
| HSA-SDS | 3.2 | 54 | 53658 | 0.35 | 160 | 370 | 1.24 |
| HRP-SDS | 6.4 | 22 | 2076 | 2.61 | 220 | 513 | 9.46 |
| HRP-DTAB | 6.4 | 45 | 3040 | 1.77 | 230 | 497 | 8.10 |
| Urease-DTAB | 10 | 310 | 3500 | 1.03 | 1890 | 268 | 5.79 |
| Urease-TTAB | 10 | 540 | 4404 | 1.54 | 2935 | 349 | 2.90 |
| Urease-HTAB | 10 | 540 | 7015 | 1.65 | 2935 | 520 | 2.56 |

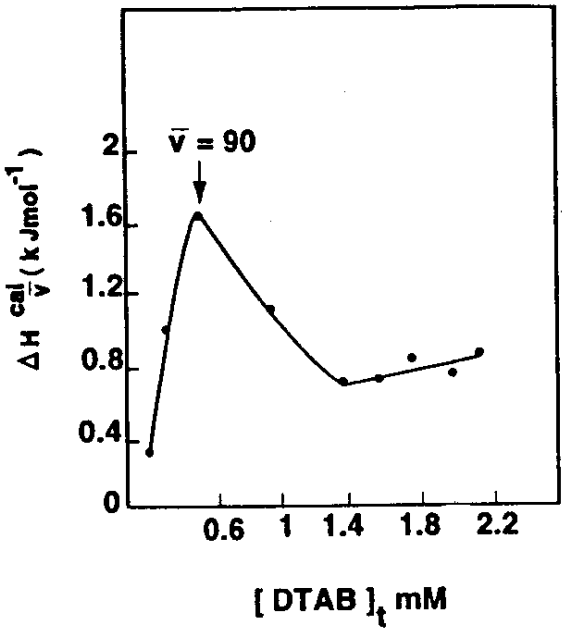


Fig. 2: Calorimetric enthalpy change per mole of protein and per mole of surfactant at pH = 8.3 and T = 27°C corresponding to DAO-DTAB interaction.

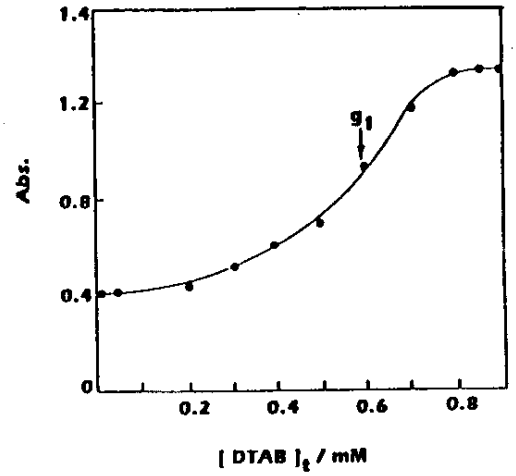


Fig. 3: The variation absorption of DAO respect to total concentration of DTAB at pH = 8.3, T = 27°C, and $\lambda_{max}$ = 280 nm.

$[DTAB]_{total}$ equal to 0.60 mM, approximately. This variation shows that the kind of binding should be changed at $\bar{v}$ equal to $g_1$ corresponding to charge neutralization at the end of electrostatic interaction.

The predominant unfolding occurs at the maximum point in the enthalpy curve. The denaturation of DAO by DTAB has been evaluated by monitoring the UV spectra change at $\lambda_{max}$= 280 nm. Figure 3 shows the absorption changes of the DAO solution in the presence of total concentrations of DTAB. The concentration midpoint of this denaturation sigmoidal curve, $[S]_{½}$, equal to 0.6 mM corresponding to $\bar{v}$ equal to $g_1$ = 90.

*HAS-SDS Ineraction*

HSA, as a mono subunit protein, has 585 amino acid residue with a molecular weight of 66,500 and three domains structure [48].

Figure 4 shows the binding isotherm for HSA-SDS interaction at pH=3.2 and temperature of 27°C. Analysis of the data according to the Hill equation indicates two sets of binding sites. The results based on a non-linear least square fitting and using equation (1) give parameters in Table 1. The first binding set, including electrostatic interaction containing 54 binding sites.

Figure 5 shows the variation in the calorimetric enthalpy of HSA-SDS interaction per

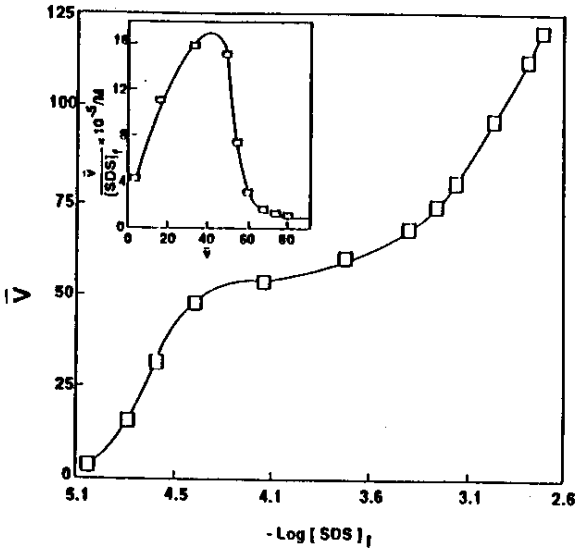


Fig. 4: Binding isotherm for HSA-SDS interaction at 27°C and pH = 3.2. Insert is Scatchard plot for this system.

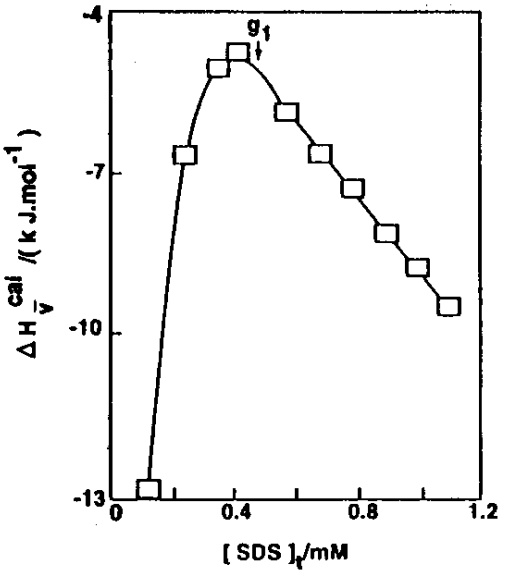


Fig. 5: Calorimetric enthalpy change per mole of protein and per mole of surfactant at pH = 3.2 and T = 27°C corresponding to HSA-SDS interaction.

mole of protein and also per mole of SDS, $\Delta H\bar{v}$ versus v. The trend of variation shows a maximum at $\bar{v} \cong g_1 = 54$ with total concentration of 1.05 mM for SDS. This maximum shows that the kind of binding should be changed at $\bar{v}$ equal to $g_1$ corresponding to charge neutralization at the end of electrostatic interaction. The predominant unfolding of HAS occurs at this maximum point in the enthalpy curve.

The denaturation of HSA by SDS has been evaluated by monitoring the UV spectra change at $\lambda_{max}$ = 278 nm. Figure 6 shows the absorption change of the HSA solution in the presence of different total concentrations of SDS. $[S]_{\frac{1}{2}}$ equal to 1.05 mM corresponding to $\bar{v}$ equal to $g_1 = 54$.

*c) HRP-DTAB Interaction*

HRP as a monomer enzyme with a molecular weight of 40,500 consists of an apoenzyme which

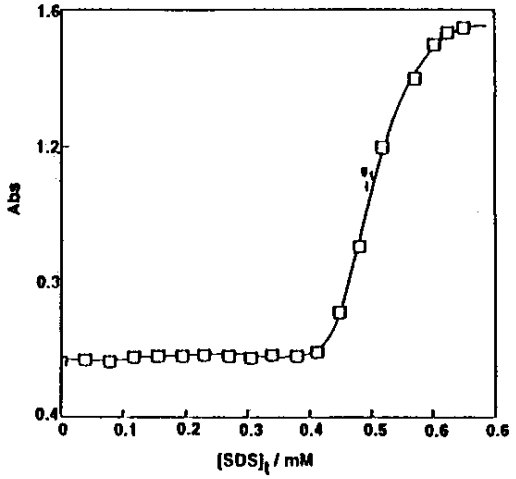


Fig. 6: The variation in absorption of HSA with respect to total concentration of SDS at pH = 3.2, T = 27°C and $\lambda_{max}$ = 278 nm.

contains both carbohydrate and protein, combined with an iron protoporphyrin IX as a non-covalently bound prosthetic group [40]. Its secondary structure with about 300 residues contains a large percent of α-helical conformation [49].

Figure 7 shows the binding isotherms for HRP-surfactant interactions at pH 6.4 and temperatures of 27 and 37°C. Analysis of these data, obtained from equilibrium dialysis, according to the Hill equation indicates two sets of binding sites. In order to fit the data to the equation (1), the values of

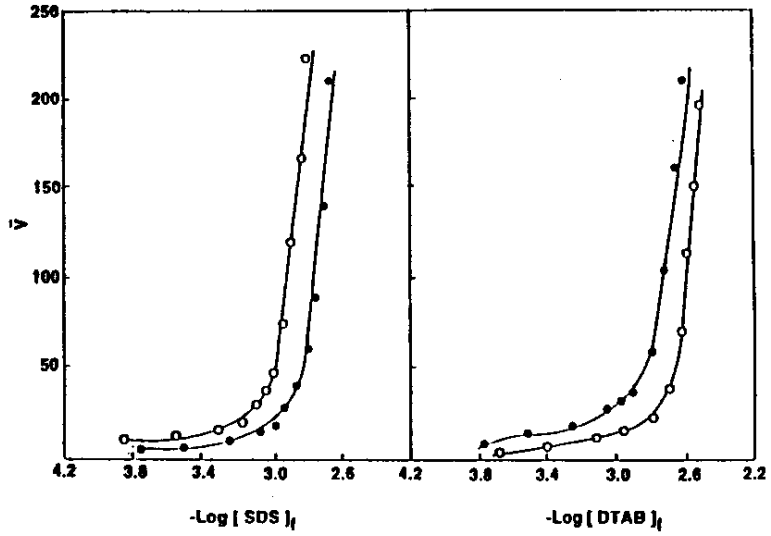


Fig. 7: Binding isotherms for HRP surfactant systems at pH 6.4 ●, 27°C; o, 37°C.

$g_1$ and $g_2$ were estimated and then the binding data were fitted to this equation using a non-linear least squares program. The results are listed in Table 1.

Figure 8 shows the sigmoidal profiles for HRP denaturation by surfactants. The upper axis in figure 8 represents $\bar{v}$ values for SDS and DTAB. These curves show the $[S]_{½}$ as the transition midpoint for denaturation profile. At this point the free energy changes is equal to zero, therefore $[S]_{½}$ is the transition midpoint for protein denaturation and saturation point for electrostatic interaction. $g_1$ is the total number of electrostatic binding sites which is coincided on $[S]_{½}$ for peroxidase appointing the two state mechanism. This technique as concurrence of $[S]_{½}$ and $g_1$ may be applied to assign the two state mechanism for other proteins in most cases.

The values of $g_1$ at 27°C and pH 6.4 for SDS and DTAB are 22 and 45, respectively (see Table 1). Also the transition concentrations under the same conditions for SDS and DTAB are 1.10 mM and 1.35 mM, respectively (see Figure 8) The enthalpy of binding ($\Delta H_{vH}$) and calorimetric enthalpy ($\Delta H_{cal}$) will be used to interpret the $[S]_{½}$ for HRP-surfactant interaction subtlety.

Binding isotherms were analysed based on the Wyman binding potential concept [50]. The binding potential is calculated from the area under the binding isotherms according to the equation.

$$\pi = RT \int_{\bar{v}_i = 0}^{\bar{v}_i} \bar{v}\, dl = \ln[S]_{free} \qquad (2)$$

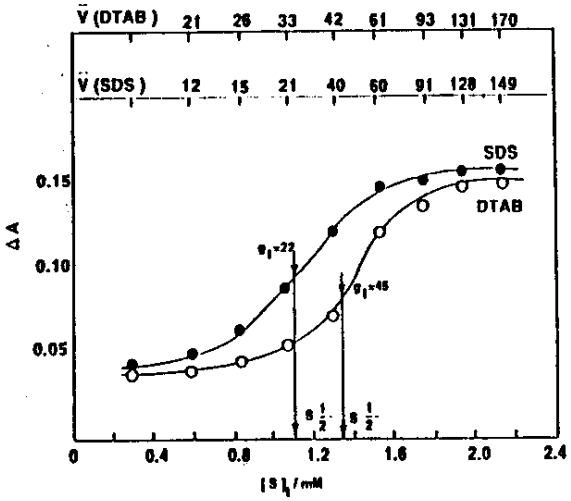


Fig. 8: Absorbance profile for SDS and DTAB on the interaction with HRP at pH 6.4 and 27°C.
●, SDS; o, DTAB

and is related to an apparent binding constant, $K_{app}$, as follows [51]:

$$\pi = RT\ln(1 + K_{app}[S]_{free}^{\bar{v}}) \quad (3)$$

The Gibbs free energy change associated with the binding process may be written as:

$$\Delta G^{\circ} = -RT\ln K_{app} \quad (4)$$

The enthalpies of binding ($\Delta H_{bin}$) were obtained from the temperature dependence of the equilibrium binding constant using the van't Hoff relations:

$$\Delta H_{bin} = -R\frac{d(\ln K_{app})}{d(1/T)} \quad (5)$$

The overall enthalpies are also determined from measurements of the enthalpy of denaturation by microcalorimetery. The overall enthalpy could be written as follows [3]:

$$\Delta H_{cal} = \Delta H_{bin} + \Delta H_{unf} \quad (7)$$

Where $\Delta H_{cal}$, $\Delta H_{bin}$ and $\Delta H_{unf}$ are calorimetric enthalpy, enthalpy of binding, and enthalpy of unfolding, respectively. By substituting the values of $\Delta H_{cal}$ and $\Delta H_{bin}$ in equation (7) enthalpy of unfolding can be obtained. Figures 9 and 10 show the changes of enthalpy values as a function of total concentration of SDS and DTAB, respectively. The figures represent an endothermic pattern for the HRP-SDS interaction, whereas an exothermic trend is observed for the HRP-DTAB interaction. Among the mentioned enthalpies, $\Delta H_{unf}$ and $\Delta H_{bin}$ characterize the interaction of HRP with surfactants. $\Delta H_{unf}$ gives the extent of unfolding raised by electrostatic interactions at transition concentration for peroxidase. As figure 11 (a,b) indicates unfolding of HRP becomes mostly complete at detergent concentrations of $[S]_{½}$, corresponding to the $g_1$ values. In other words, the unfolding process depends on the ionic interactions, and the enthalpy of unfolding at $g_1$ points involve 95 and 97 percent of the related overall unfolding enthalpies for SDS and DTAB, respectively. This means that the hydrophobic

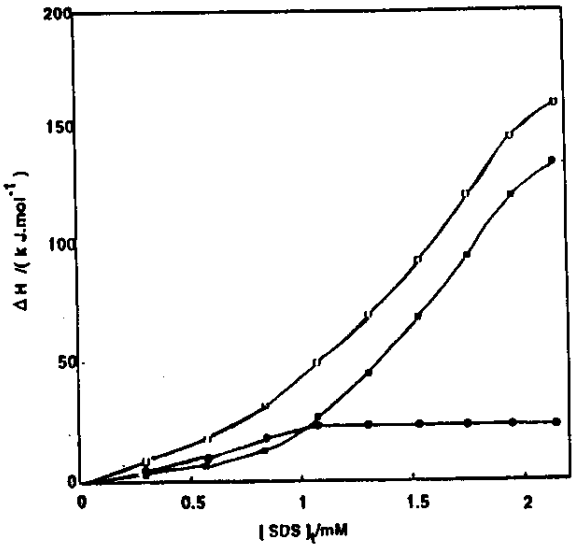


Fig. 9: Enthalpy changes on the interaction of HRP with SDS at pH 6.4 and 27oC.
□, calorimetric; ■, binding ; ●, unfolding

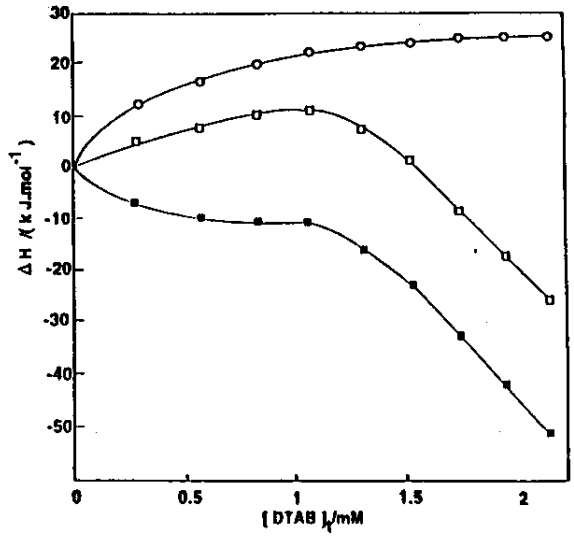


Fig. 10: Enthalpy changes on the interaction of HRP with DTAB at pH 6.4 and 27°C.
□ calrimetric■binding;● unfolding

interactions contribute to a smaller extent in unfolding of HRP by the surfactants, whereas urea and guanidine hydrochloride as chemical denaturants indicate a large contribution of hydrophobic interactions in the unfolding of HRP [13].

Figure 11 (a,b) also shows the dependence of $\Delta H_{bin}$ ($\bar{\nu}$) on $\bar{\nu}$ $\Delta H_{bin}$ ($\bar{\nu}$) is an approximate value of $\Delta H_{bin}$ due to binding of one mole of surfactant to one mole of HRP at the corresponding $\bar{\nu}$ value ($\Delta H_{bin}/\bar{\nu}$). The maxima and minima on the $\Delta H_{bin}$ curves show the coincidence of $g_1$,$[S]_{½}$ and saturation point at $\Delta H_{unf}$ curve. This appearance means that the $[S]_{½}$ point is the position of the end of ionic interaction and start of hydrophobic contribution. Although the binding of surfactants continues at $\bar{\nu}>g_1$ but the unfolding process of HRP was mostly completed by first set of anionic and cationic detergents. Thus, $\Delta H_{bin}(\bar{\nu})$ could be introduced as a subtle parameter for a clear indication of transition concentration ($[S]_{½}$) or the saturation point of ionic binding sites ($g_1$) for the interaction of HRP with ionic surfactants. The electrostatic (for $\bar{\nu}<g_1$) and the hydrophobic (for $\bar{\nu}>g_1$) portions are separated from each other by this parameter.

*Urease-Cationic surfactant interaction:*

Urease, the first enzyme to be crystallized [52] and the first shown to include nickel [53], catalyzed the hydrolysis of urea [54]. Jack bean

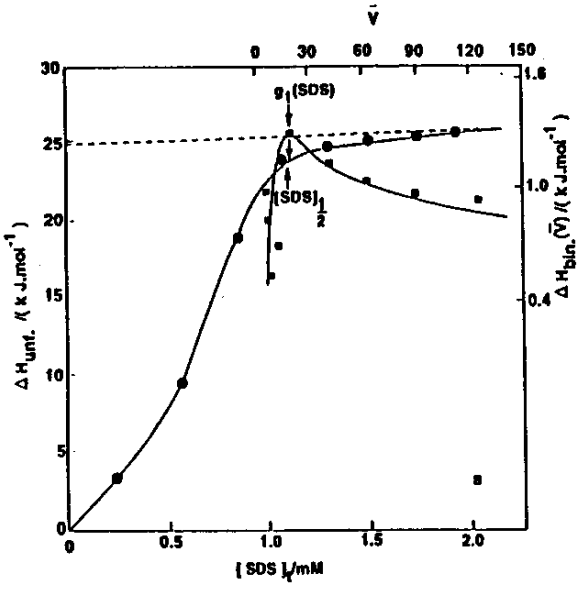


Fig. 11a: ●, Dependence of $Dh_{unf}$ of HRP on the total concentration of SD;■, plot of $\Delta H_{bin}$ ($\bar{\nu}$) vs, $\bar{\nu}$ (SDS) at pH 6.4 and 27°C.

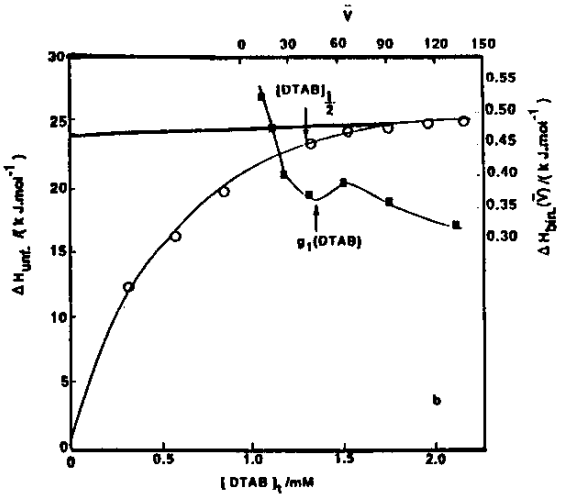


Fig. 11b: ● , Dependence of $\Delta H_{unf}$ of HRP on the total concentration of DTAB;■, plot of $\Delta H_{bin}$ ($\bar{\nu}$) vs, $\bar{\nu}$ (DTAB) at pH 6.4 and 27°C.

urease has six identical subunits with molecular weight of 545, 340 Da including two nickel ions per its only active site in each subunit [55]. Each subunit has 840 amino acids residue [55].

The binding isotherms have been plotted as the average number of bound surfactants to one macromolecule, ($\bar{\nu}$) vs.log$[S]_f$, as shown in Fig. 12. It shows the binding isotherms for the binding of DTAB, TTAB, and HTAB with jack-bean urease at pH = 10 and 27°C.

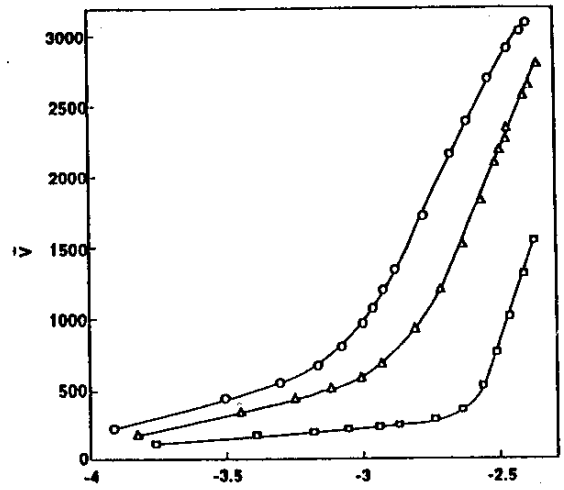


Fig. 12: Binding isotherms for binding jack bean urease with DTAB (□), TTAB (Δ), and HTAB (○) at pH = 10 and 27°C.

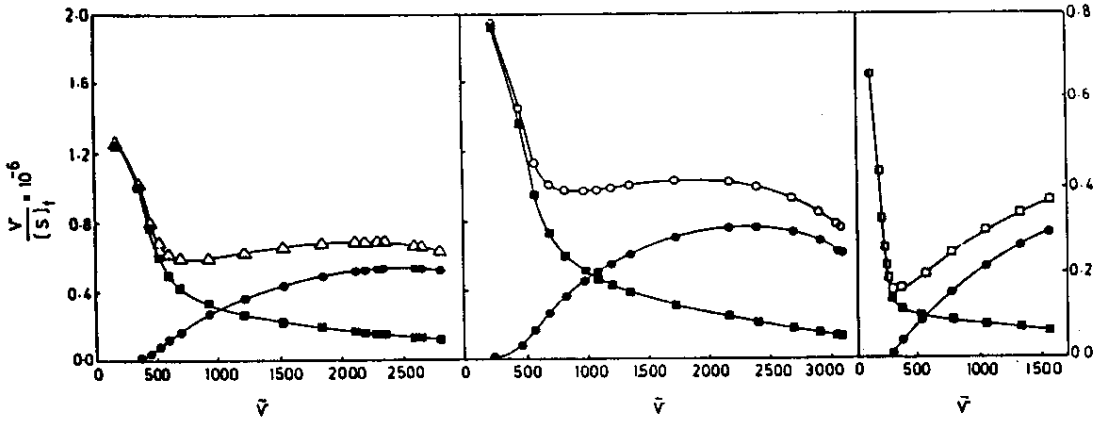


Fig. 13: The Scatchard plots for binding jack bean urease with DTAB (▫), TTAB (Δ), and HYA (○) at pH = 10 and 27°C. Non-linear Scatchard plot of the same data resolved into two types of binding the first binding sites (■) and the second binding sites (●). The right scale is ordinate-axis for DTAB.

The Scatchard plots are shown in Fig. 13. These unusual cases may be due to the nature of the interactions between ionic surfactants and proteins which have an amphipathic property. Thus this system may be considered with two sets of binding sites, including an electrostatic interaction and a hydrophobic interaction. The data for the binding of DTAB, TTAB, and HTAB to urease have been fitted to Eq.(1) using a computer program for non-linear least-square fitting (tabulated in Table 1).

The absorption changes of the urease solution at $\lambda_{max}$= 278 nm in the presence of different concentrations of surfactants is shown in Fig. 14. The values of $\bar{v}$ in each total concentration of the surfactant were calculated from Fig. 12, using the following equation.

$$[\text{surfactant}]_{total} = [\text{surfactant}]_{free} + \bar{v}\,[\text{urease}]_{total} \quad (8)$$

The sigmoidal curves of denaturation given in Fig. 14 were obtained in the concentration range of the electrostatic interaction ($\bar{v} < g_1$). It is important to note that more than 90% unfolding of urease occurs in this concentration range [3]. The values of $\Delta H_{unf}$ in the first and second steps are 6550 and 650 kj.mol$^{-1}$, respectively [3]. This might be due to the fact that the electrostatic interaction perturbs the charge balance at the surface of the protein.

Figure 15 shows the variation in the calorimetric enthalpy per mole of protein, which has been divided to $\bar{v}$; $\Delta H_{\bar{v}} = \Delta H/\bar{v}$, with respect to the total concentration of the surfactant. The calorimetric enthalpy involves the heat of surfactant binding to the protein and the heat of protein unfolding. The interactions of DTAB and TTAB are exothermic, while HTAB is endothermic. However, the exothermicity of DTAB, especially at higher values of v, is more than that of TTAB.

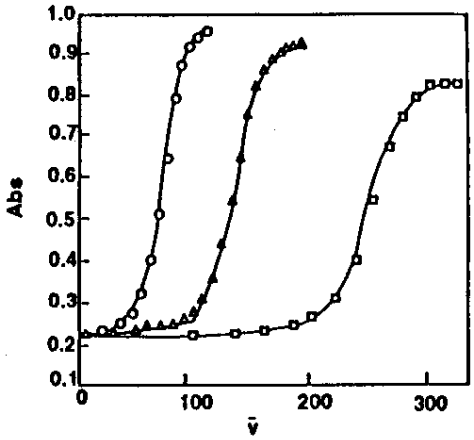


Fig. 14: The variation of absorption with respect to $\bar{v}$ for jack bean urease (0.026% w/v) with DTAB(▫) TTAB (Δ), and HTAB(○) at pH = 10, T = 27°C and $\lambda_{max}$ = 278 nm.

The enthalpy curves of DTAB and TTAB have a distinct minimum, which could be due to an endothermic process during an exothermic process.

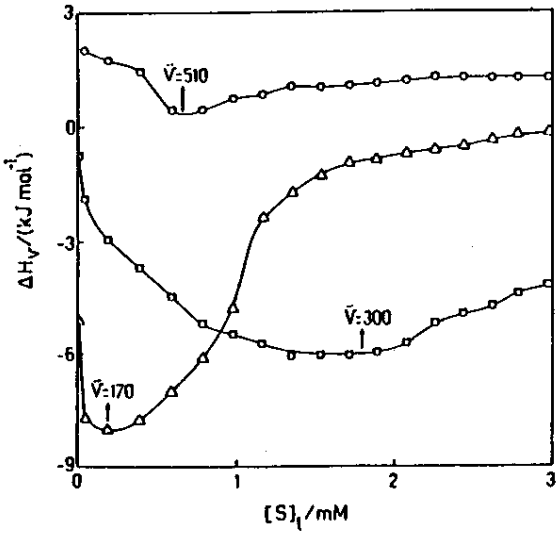


Fig. 15: The variation of calorimetric enthalpy per mole of protein and per mole of surfactant ($\Delta H\bar{v}$) respect to total concentration of DTAB (□), TTB (Δ), and HTAB (○) and HTAB (●) at pH = 10 and T = 27°C. The urease concentration was 0.006% (w/v).

These minima points occur at v equal to 300 and 170 for DTAB and TTAB, respectively. In addition, these appearance are along with predominant unfolding of the protein according to the spectroscopic data (Fig 14). The unfolding of the protein (endothermic process ) and the change in the kind of binding from electrostatic (exothermic process) to pure hydrophobic interactions (endothermic process) lead to a minimum in the enthalpy curves of DTAB and TTAB. The large difference in $\bar{v}$ at the minimum point of the enthalpy curve with $g_1$ for TTAB, with respect to DTAB. This fact shows the preliminary interaction due to the hydrophobic tail of the surfactant with hydrophobic patches at the surface of the protein, which accompanies an electrostatic interaction of cationic heads of the surfactant with anionic amino acids at the surface of the protein. These neutralizations perturb the force balance in protein structure and ultimately the denaturation of the protein.

Figure 15 shows a distinct minima for the interaction of HTAB with urease. This point occurs at $\bar{v} = g_1 = 510$, showing the change in the kind of binding. This has certified our binding data analysis in terms of two sets of binding sites. However, a spectroscopic denaturation study (Fig. 14) indicates that the predominant unfolding of urease occurs at $\bar{v}$ = 90, which is much lower than $g_1$. It is consistent with our above discussion concering the role of the length of the surfactant tail in the denaturation strength. The calorimetric enthalpy curve of the HTAB-urease interaction (Fig. 15) does not show the status of the enthalpy interaction below $\bar{v}$ = 90, because urease was denatured by the first injection of HTAB into the protein solution.

The spectroscopic and calorimetric studies show that the predominant unfolding occurs at a region where the first binding set occurrs, and that the strength of denaturation of the surfactants increases by the increase in length of the hydrophobic tail. The values of $[S]_{½}$ for DTAB, TTAB and HTAB are 1.4, 0.15 and 0.044 mM, respectively. The increase in the denaturation strength of the surfactant with increasing the tail length is related to preliminary hydrophobic interactions of the surfactant tail with hydrophobic patches, which are accompanied by a neutralization of the charge at the surface of the protein. The electrostatic interaction follows the preliminary hydrophobic interactions by a more extensive pure hydrophobic interaction.

It is important to note there that there is no coincadence between $[S]_{1/2}$ and $g_1$ because of multistate mechanism for Urease unfolding as six subunit protein.

## Experimental

*Materials*

D-amino acid oxidase (E.C. 1.4.3.3,DAO), horseradish peroxidase (E.C. 1.11.1.7, HRP) jack bean urease (E.C. 3.5.1.5), human serum albumin (essentially fatty acid free, HSA) sodium n-dodecyl sulphate (SDS), dodecyl trimethylammonium bromide (DTAB), tetradecyl trimethylammonium bromide (TTAB), hexadecyl trimethylammonium bromide (HTAB), Orange II dye and rosaniline were obtained from Sigma Chemical Co.

Visking membrane dialysis tubing (MW cut-off 10,000-14,000) was obtained from Scientific Instrument Center Ltd. (SIC, Eastleigh, Hampshire, U.K).

All materials and reagents were of analytical grades, and solutions were made in double-distilled water. Glycine solutions (50 mM), pH=3.2 and pH=10, sodium phosphate solution (2.5 mM), pH=6.4, and pyrophosphate solution (50 mM) pH=8.3, have been used as buffers.

*Methods*

*Equilibrium dialysis*

Experiments were carried out at 300 K using a protein solution with a concentration of 0.04%(w/v) of DAO, 0.02%(w/v) of HRP, 0.1%(w/v) of HSA and 0.5% of urease, of which 2 ml aliquots were placed in dialysis bags and equilibrated with 2 ml of the surfactants solutions, covering the required concentrations range for over 96h. The free DTAB, TTAB and HTAB concentrations in equilibrium with complexes were assayed by the orange II methods [37]. The free SDS concentrations in equilibrium with complexes were assayed by the rosaniline method [38]. The molecular weight of DAO, HRP, HSA, and urease were taken to be 76000 [39], 40,500[40], 66,500 [41], and 545,340 [42,43], respectively.

*Spectrophotometry*

These experiments were performed using a recording spectrophotometer (UV-3100 Shimadzu model, Japan). The sample cell contained 2 ml of a protein solution at a certain concentration with different fixed concentrations of the surfactant. The reference cell was excluded of protein. Both of the cells were set at a constant temperature. The absorption of the sample cells was recorded at protein specific maximum wavelength ($\lambda_{max}$) versus the reference cells.

*Isothermal Titration Microcalorimetry*

The microcalorimetric experiments were carried out with a four-channel commercial microcalorimetric system (Thermal activity Monitor 2277, Thermometric, Sweden). Each channel is a twin heat-conduction calorimeter where the heat-flow sensor is a semi conducting thermopile (multijunction thermocouple plates) positioned between the vessel holders and the surrounding heat sink. The insertion vessel was made from stainless steel. Surfactant solution (20 mM) was injected by use of a Hamilton syringe into the calorimetric stirred titration vessel, which contained 2 ml protein solution with certain initial concentration. Thin (0.15 mm inner diameter) stainless steel hypodermic needles, permanently fixed to the syringe, reached directly into the calorimeter vessel. The injection of surfactant into the perfusion vessel was repeated several times. The calorimetric signal was measured with a digital voltmeter, part of a computerized recording system. The enthalpy change for each injection was calculated by "Digitam" computer program. The enthalpy of dilution and demicellization of the surfactant solution were measured as described above, except that the protein was excluded. The enthalpy of dilution and demicellization for surfactant micelles was subtracted from the enthalpy of protein-surfactant interaction. The enthalpy of dilution of protein is also negligible. The microcalorimeter was calibrated electrically frequently during the course of the study.

## Conclusion

Surfactants combine with most native proteins directly in multiple equilibria causing denaturation of proteins. With respect to the amphipathic nature of surfactatns and proteins, it is established that there are two kinds of interactions in the binding of ionic surfactants to proteins. The electrostatic interaction is accompanied by preliminary hydrophobic interactions which occurrs initially, followed by a more extensive pure hydrophobic interaction. The predominant unfolding of the protein occurs at a region where the first binding set is present due to neutralizations, perturbing the force balance in protein structure. The distinction of electrostatic and hydrophobic proteins in protein-surfactant interaction by two set analysis theory prevail the following cases:

The coincidence of $[S]_{\frac{1}{2}}$ and $g_1$ suggests a two state unfolding mechanism for small globular proteins.

Finding the enthalpy and energy and the quantity contribution of electrostatic and hydrophobic forces in protein unfolding will be of interest.

## References

1. C. Tanford, *Adv. Protein Chem.*, **24**, 1, (1970).
2. A.A. Moosavi-Movahedi, *J. Sci. I.R. Iran*, **4**, 247, (1993).
3. A.A. Saboury, A.K. Bordbar and A.A. Moosavi-

Movahedi, *J. Chem. Thermodynamics,* **28**, 1077, (1996).
4. A.A. Saboury and A.A. Moosavi-Movahedi, *Bochem. Education,* **23**, 164, (1995).
5. E.C. Row and C. Tanford, *Biochemistry,* **24**, 4822, (1973).
6. S. Lapanje, "Physico-chemical Aspects of Protein Denaturation", Wiley, New York, Chapters 1, 4, (1978).
7. M.N. Jones, "Biological Interfaces" Elsevier, Amesterdam, Chapter 5, (1975).
8. W. Pfeil "Biochemical Thermodynamics" second edition (edited by M.N. Jones), Elsevier, Amesterdam, 53-92, (1988).
9. C.N. Pace, *TIBTECH,* **8**, 93, (1990).
10. A.A. Moosavi-Movahedi, M.R. Razeghifard, M.M. Farajollahi and M. Zahmatkesh, *Thermochimica Acta,* **219**, 151, (1993).
11. P.L. Privalov, *Biochemistry and Molecular Biology,* **25**, 281, (1990).
12. A.A. Moosavi-Movahedi,, G.A. Naderi and B. Farzami, *Thermochimica Acta,* **239**, 61, (1994).
13. A.A. Moosavi-Movahedi and K. Nazari, *Int.J. Biol. Macromol.*, **17**, 43, (1995).
14. A.A. Moosavi-Movahedi and M.R. Housain-dokht, *J. Sci. I.R. Iran,* **1**, 253, (1990).
15. A. A. Saboury, A.K. Bordbar and A.A. Moosavi-Movahedi, *Bull. Chem. Soc. Jpn.*, in press (1996).
16. M.N. Jones, *Chem. Soc. Rev.*, **21**, 127, 1992.
17. A.A. Moosavi-Movahedi, *Pure and Appl. Chem.*, **66**, 71, (1994).
18. A.A. Moosavi-Movahedi and M.R. Housain-dokht, *Int. J. Biol. Macromol.*, 13, 50, (1991).
19. A.A. Moosavi-Movahedi and M.R. Housain-dokht, *Int. J. Biol. Macromol.*, **16**, 77, (1994).
20. S.N. Timasheff and T. Arakawa, Protein Structure, IRL Press at Oxford University Press, England, chapter 14, (1990).
21. C.A. Nelson, *J. Biol. Chem.*, **246**, 3895, (1971).
22. M.N. Jones, P. Manley, P.J.W. Midgley and A.E. Wilkinson, *Biopolymers*, **21**, 1435, (1982).
23. M.N. Jones, A. Finn, A.A. Moosavi-Movahedi and B.J. Walker, *Biochem. Biophys. Acta*, **913**, 395, (1987).
24. M.L. Anson, *J. Gen. Physiol.*, **23**, 239, (1939).
25. A.A. Moosavi-Movahedi, M.N. Jones and G. Pilcher, *Int. J. Biol. Macromol.*, **10**, 75, (1988).
26. A.A. Moosavi-Movahedi, M.N. Jones and G. Pilcher, *Int. J. Biol. Macromol.*, **11**, 26, (1989).
27. G. Prieto, J.M. del Rio, M.I. Paz Andrade, F. Sarmiento and M.N. Jones, *Int. J. Biol. Macromol.*, **15**, 343, (1993).
28. J.A. Raynold, S. Herbert, H. Polet and J. Steinhardt, *Biochemistry,* **6**, 937, (1967).
29. E. Tipping, M.N. Jones and H.A. Skinner, *J. Chem. Soc., Faraday Trans*, **70**, 1306, (1974).
30. G. Scatchard, *Ann. N.Y. Acad. Sci.*, **51**, 660, (1949).
31. A.A. Saboury and A.A. Moosavi-Movahedi, *Biochem. Education,* **22**, 48, (1994).
32. A.K. Bordbar, A.A. Saboury and A.A. Moosavi-Movahedi, *Biochem. Education,* **24**, 172, (1996).
33. I.M. Klotz. The proteins (Edited by H. Neurath and K. Bailey), Vol. 1: Academic Press, New York 727-806, (1953).
34. I.M. Klotz, *Science,* **217**, 1247, (1982).
35. A.V. Hill, *J. Physiol.*, **40**, iv-vii, (1910).
36. J. Wyman, *Adv. Protein Chem.*, **4**, 407, (1938).
37. A.V. Few and R.H. Ottewill, *J. Colloid Sci.*, **11**, 34, (1956).
38. F. Karush and M. Sonnenberg, *Anal. Chem.*, **22**, 175, (1950).
39. S.C. Tu and D.B. Mc Cormic, *J. Biol. Chem.*, **248**, 6339, (1973).
40. D. Keglin and E.F. Hartree, *Biochem. J.*, **49**, 88, (1951).
41. C.C. Daniel, *Science*, **244**, 1195, (1989).
42. R.P. Hausinger "Biochemistry of Nickel" Plenum Press, New York, page 23, (1993).
43. K. Takishima, T. Suga and G. Mamia, *Eur. J. Biochem.*, **175**, 151, (1988).
44. B. Cuti and S. Ronchi, *Biochem. Biophys. Acta*, **248**, 633, (1973).
45. K. Shiga and T. Shiga, *Arch. Biochem. Biophys.*, **145**, 701, (1971).
46. R.S. Swenson and V.J. Massey, *J. Biol. Chem.*, **25**, 5602, (1982).
47. M.L. James, G.M. Smith and J.C. Wolford, Applied numerical methods for digital computer, 3rd ed. Harper and Row Publisher. New York (1985).
48. D.C. Carter, *Sciecne*, **244**, 1195, (1989).
49. E.H. Strickland, E. Kay, L.M. Shannon and J. Horwitz, *J. Biol. Chem.*, **243**, 3560, (1965).
50. J. Wyman, *J. Mol. Biol.*, **11**, 631, (1965).
51. M.N. Jones and P. Manley, *J. Chem. Soc.*

*Faraday Trans 1*,77, 827, (1981).
52. J.B. Sumner, *J. Biol. Chem.*, **69**, 435, (1926).
53. N.E. Dixon, C. Gazzola, R.E. Blakeley and B. Zerner, *J. Am. Chem. Soc.*, **97**, 4131, (1975).
54. H.L.T. Mobley and R.P. Hausinger, *Microbiol. Rev.*, **53**, 85, (1989).
55. K. Takishima, T. Suga and G. Mamia, *Eur. J. Biochem.*, **175**, 151, (1988).